Study of diluted magnetic semiconductor: Co-doped ZnO

Hyeon-Jun Lee and Se-Young Jeong[a)]
Department of Physics, Pusan National University, Busan 609-735, Korea and COMTECS Limited, Advanced Materials Research Laboratory, Daegu 704-702, Korea

Chae Ryong Cho
Korea Basic Science Institute, Busan branch, Busan 609-735, Korea

Chul Hong Park
Research Center for Dielectric and Advanced Matter Physics, Pusan National University, Busan 609-735, Korea

(Received 8 July 2002; accepted 4 September 2002)

We report on the high-temperature ferromagnetism in Co-doped ZnO films fabricated by the sol–gel method above 350 K. The lattice constant of c axis of wurtzite $Zn_{1-x}Co_xO$ follows Vergard's law for $0<x<0.25$. For $Zn_{1-x}Co_xO$ with $x \geqslant 0.25$, a secondary phase is detected. The $Zn_{1-x}Co_xO$ exhibits ferromagnetic behavior with a Curie temperature higher than 350 K. By the results of x-ray photoelectron spectroscopy measurement, we assume that Co occupied the Zn site without changing the wurtzite structure. In the case of $x=0.2$, the coercive field measured by a magnetization–magnetic field hysteresis curve at 350 K was nearly 80 Oe. Additionally, we investigated the electric structure through first-principles pseudopotential plane-wave calculation. © *2002 American Institute of Physics.* [DOI: 10.1063/1.1517405]

Diluted magnetic semiconductors (DMS) have been of much interest and have been studied actively for the purpose of the use of both charge and spin of electrons in semiconductors. Spin injection into non-magnetic semiconductors was tried by many research groups due to the potential to create new classes of spintronics devices. Previous efforts were focused on the direct electrical injection of spin-polarized electrons using a ferromagnetic metal-coated on metal–semiconductor junction.[1] However, these effects suffer from the scattering of the spin-polarized carrier at the Schottky barrier of the metal–semiconductor interface, called the "*dead layer*." In order to overcome the dead layer, recent advances in spin polarization came from the introduction of DMS.[2]

DMS are semiconductors in which transition-metal ions substitute cations of the host semiconductor materials. Localized d electrons of the magnetic ions couple with the extended electrons in the semiconducting band. These couplings lead to a number of peculiar and interesting properties, such as magneto-optical and magneto-electrical effects. Dietl *et al.*[3,4] suggested GaN and ZnO as candidates having a high T_c and a large magnetization, and lately a few experimental results were reported.[5–9] $Zn_{1-x}Co_xO$ is interesting not only in terms of its room-temperature ferromagnetism,[6] but also in its ferromagnetic transport properties. In addition, Sato *et al.*[10] suggested theoretically that the ferromagnetic state in Mn-, Fe-, Co-, and Ni-doped ZnO-DMS can be stabilized. Ueda *et al.*[5] reported the ferromagnetic behaviors with a Curie temperature higher than room temperature for the Co-doped ZnO films grown by the pulsed-laser deposition technique, but its reproducibility was less than 10%. Jin *et al.*[9] had found no indication of ferromagnetism in films grown by laser molecular-beam epitaxy. Cho *et al.*[8] reported the ferromagnetism for the CoFe-doped ZnO and FeCu-doped ZnO films, respectively. In this letter, we report on ferromagnetism in sol–gel processed $Zn_{1-x}Co_xO$ powder and its films. The sol–gel method has some advantages in fabricating DMS samples, because one can control the mole fraction accurately, easily fabricate samples with various compositions, and increase the solubility.

$Zn_{1-x}Co_xO$ thin films were grown on (0001) Al_2O_3 substrate. Zinc acetate and cobalt acetate were dissolved in 2-methoxyethanol solutions and a solution of 0.5 mol/l was prepared. The coating solution was dropped and spin coated with 3000 rpm for 30 s in air. This process made a precursor film on the substrate. The precursor film specimen dried at 300 °C in air for 10 s. We performed 12 coatings of Co-doped ZnO precursor by spincoating with increasing Co con-

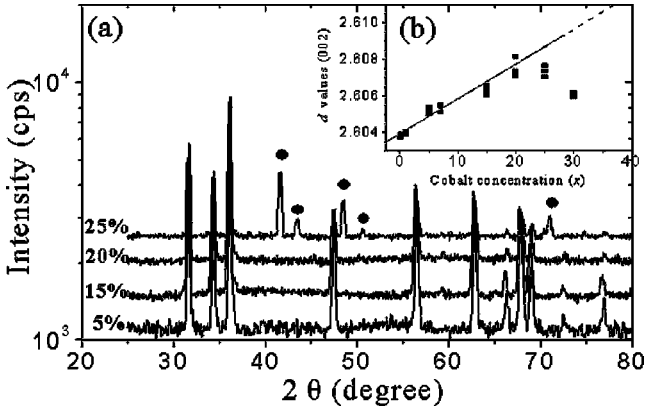

FIG. 1. (a) θ–2θ XRD pattern (logarithmic scale) of Co-doped ZnO films in powder. These marks (●) indicated that the peaks are not ZnO patterns. (b) Cobalt content (x) dependency of the lattice constants c of Co-doped ZnO. The square dot and solid line indicate the results of XRD and Vegard's law.

a)Author to whom correspondence should be addressed; electronic mail: syjeong@pusan.ac.kr

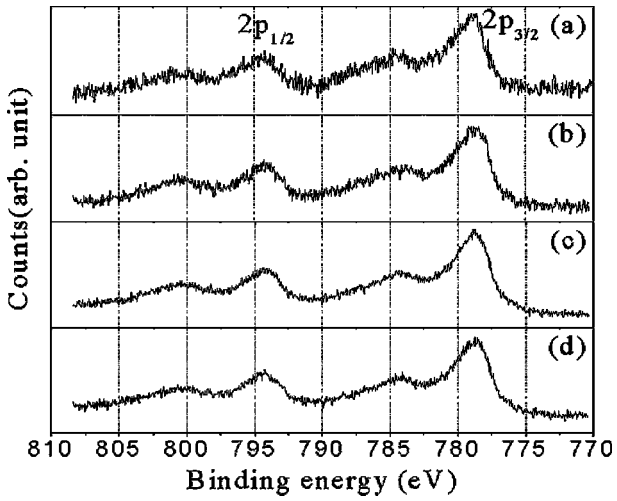

FIG. 2. XPS studies of Co $2p_{3/2}$ and $2p_{1/2}$ peaks for Co-doped ZnO films (a) 5%, (b) 10%, (c) 20%, and (d) 25%.

centration (0%, 0.5%, 0.7%, 1%, 5%, 7%, 10%, 15%, 20%, 25%, and 30%) and annealed under an O_2 environment using the rapid thermal annealer at 700 °C for 1 min. The thickness of the Co-doped ZnO film was measured to be 2000–2500 Å for a scanning electron microscope cross-sectional image.

Characterization of Co-doped ZnO films by x-ray diffraction (XRD) was performed using monochromic Cu $K\alpha$ radiation ($\lambda = 1.5405$ Å) operated at 40 kV and 80 mA. The films were also characterized by x-ray photoemission spectroscopy (XPS) using Al K radiation ($h\nu = 1486.6$ eV). A superconducting quantum interference device [(SQUID) Quantum Design] was used to investigate the magnetic properties of these samples. In order to get a maximum magnetic signal from the $Zn_{1-x}Co_xO$ films, five pieces of films were piled up perpendicularly to a magnetic field. Hall effects were measured using the four-point probe method at 77 K and 300 K.

The crystal structures of Co-doped ZnO were characterized by XRD. We observed c-axis oriented peaks for the thin film sample. We examined whether cobalt clusters are formed during the process, and whether Bragg peaks of impurities are observed. We present the data for the powder samples. The typical XRD patterns of Co-doped ZnO powder are shown as a logarithmic scale in Fig. 1(a). The subsequent XRD showed that the doping does not change the wurtzite structure of ZnO for doping concentrations below 25% and, furthermore, we could not find any Co cluster in the XRD measurement. Above 25%, some undefined peaks (●) appeared, which were not the peaks of either Co_2O_3 or Co_3O_4. The diffraction pattern reveals only the presence of the peaks corresponding to hexagonal ZnO and no second phase peaks. But the results of these data do not mean there is an absence of Co clusters. We do not exclude the possibility of the formation of clusters small enough not to be detected in XRD. The lattice constants of the c axis ($d(002)$ value) increase with x of $Zn_{1-x}Co_xO$ as shown in Fig. 1(b). The solid line in Fig. 1(b) is a plotting line using the Vegard law. The d values increase with increasing cobalt content up to 25% and they tend to obey the Vegard law. However, the d value decreases above 25%. It is noted that the solubility of Co exceeds a thermal equilibrium limit below 25% due to a no-equilibrium sol–gel process.

It was ascertained using XPS studies that the Co ion in the ferromagnetic $Zn_{1-x}Co_xO$ wurtzite structure is in the 2 + formal oxidation state, as shown in Fig. 2. The charge-shifted spectra were corrected using the adventitious C 1s photoelectron signal at 285 eV. Here, we show the Co $2p_{3/2}$ core levels for Co—O bonding at 779.02 eV, and the energy difference between Co $2p_{3/2}$ and Co $2p_{1/2}$ is 15.47 eV. This excludes the possibility of the formation of a Co cluster, since, if Co exists as metal cluster itself in the thin films, the energy difference should be 15.05 eV. On the other hand, if Co is surrounded by oxygen, these differences should be 15.5 eV.[11] The valence of Co is not easily determined by XPS. However, formation of Co metal cluster in our samples can be ruled out.[12]

We investigated the magnetic properties of these samples using SQUID. Figure 3(a) shows the temperature dependence of the magnetization ($M-T$ curve) of $Zn_{1-x}Co_xO$ films with $x = 5\%$, 10%, 20%, and 25% between 5 and 350 K, where a 500 Oe magnetic field is applied. This trend is similar to paramagnetic behavior, but the ferromagnetic hysteresis loop was observed in the whole temperature range.[13] The magnetization decreases rapidly up to 25 K for all samples and increased[7] slowly with increasing temperature above 25 K. The increment of the magnetization with increasing temperatures seems to be caused by the increasing of the electron carrier concentrations (Table I). The magnetization increased with an increase of Co concentration. The $M-H$ curve (field dependence of magnetization) of Co-doped ZnO films measured at 350 K showed hysteresis loops with the coercive field (H_c) of 80 Oe in 20% doped sample, as shown in Fig. 3(b). The saturation magnetization of the film is estimated to be $0.56 \pm 0.1\ \mu_B$/Co site from the $M-H$ curve at 350 K. In 5%, 10%, and 20% doped samples, the magnetizations decreased with an increasing magnetic field above the saturated magnetic field, because of the diamagne-

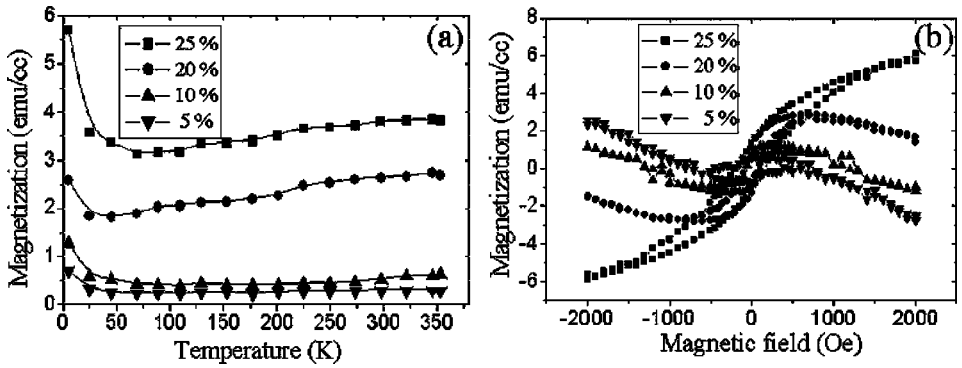

FIG. 3. (a) Temperature dependence of magnetization in 500 Oe and (b) hysteresis curves measured at 350 K for Co-doped ZnO film.

TABLE I. Carrier concentration [10^{17} cm^{-3}] and resistance [Ω cm] at 77 K and 300 K using the Hall effect. L indicates 77 K; R, 300 K.

	ZnO(0%)	ZnCoO(5%)	ZnCoO(20%)
concentration^L	6.28	4.92	1.29
concentration^R	18.4	9.51	5.25
resistance^L	0.027	4.80	6.75
resistance^R	0.030	0.92	1.50

tism of the substrate (Al_2O_3).[6] These $M-T$ and $M-H$ curves indicate that the films processed by the sol–gel method clearly show ferromagnetism even above 350 K.

The resistances and carrier concentrations measured using the Hall effect at 77 K and 300 K for pure ZnO and Co-doped ZnO are given in Table I. The types of films used were found to be n type with electron concentration of 10^{17} cm^{-3}. The resistance of pure ZnO and Co-doped ZnO at 77 K are very large even at 300 K. This indicates that $Zn_{1-x}Co_xO$ samples show an insulating behavior. Additionally, $Zn_{1-0.05}Co_{0.05}O$ showed two orders of magnitude larger resistance than in pure ZnO films. In particular, the carrier concentration of Co-doped ZnO increased with increasing temperature. These results correspond to increasing magnetization with an increasing of temperature in Fig. 3(a). This result can be explained using the electronic structure.

We investigate the electronic structure of ZnCoO through the first-principles pseudopotential plane-wave calculation within the local spin density approximation.[14] The pseudopotentials were generated in the manner of Troullier and Martins.[15] The energy cutoff of 60 Ry was used for the plane-wave expansion. The atomic geometry is fully relaxed by calculating the Hellmann–Feynman forces. A periodic supercell with 16 atoms includes one Co atom. The calculated density of states are shown in Fig. 4. The Co-d orbital of majority spin is located mainly 5.4 eV below the valence band maximum (VBM) and strongly hybridized with host sp orbitals. The location of the d level is estimated to be lower by about 3 eV compared to other Koringa–Kohn–Rostoker-CPA calculations. The Co-d state of minority spin are occupied by two electrons. The energy levels are located within the band gap. The two-fold degenerated lowest level of the Co-d e_g states the three-fold upper levels t_{2g} state are located 0.6 eV and 2.2 eV, respectively, above the VBM. The

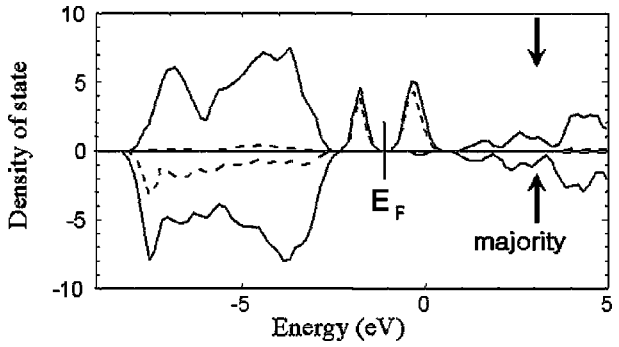

FIG. 4. Total density of states (solid line) and local density of Co-d state-(dashed line) in Co-doped ZnO.

lower e_g states are fully occupied. The upper levels are empty and thus the Co in ZnO makes deep impurity levels. It is well known that the donorlike defects such as oxygen vacancy and Zn interstitial are easily formed in ZnO, which leads to the natural n-type doping.[16] The Co impurity deep levels can "*trap*" the electrons emitted by donorlike defects such as oxygen vacancy and Zn interstititals. The trapping of electron may induce the ferromagnetic spin–spin interaction between Co atoms.[17] It also increases the resistance due to the decrease of the carrier densities.

In summary, we have characterized $Zn_{1-x}Co_xO$ powder and thin films fabricated by the sol–gel process and found that the lattice constants increase with increasing Co concentrations. Below 25%, no secondary phase was observed in our sol–gel process, and the solubility of Co in ZnO exceeds a thermal equilibrium limit below 25%. From the results of XPS, doped Co is homogeneously surrounded by oxygens. The Co-doped ZnO thin film showed ferromagnetism above 350 K. The Ueda *et al.*[5] group reported this ferromagnetism, but with low reproducibility. Cho *et al.*[8] reported $Zn_{1-x}(Co_{0.5}Fe_{0.5})_xO$ and could enhance the ferromagnetism. However, in our study, we could observe ferromagnetism above 350 K without any additional doping. The controversial results between research groups suggest that the ferromagnetism strongly depends on the technical method for the fabrication of the samples. In further work, we will study the II–VI and III–V families in order to interpret the origin in DMS.

This work was supported by Grant No. R14-2002-029-01000-0 from ABRL prgram of KOSEF and partially supported by KOSEF via electron Spin Science Center at POSTECH.

[1] J. F. Gregg, W. D. Allen, N. Viart, R. Kirschman, C. Sirisathitkul, J.-P. Schille, M. Gester, S. M. Thompson, P. Sparks, V. da Costa, K. Ounadjela, and M. Skvarla, J. Magn. Magn. Mater. **175**, 1 (1997).
[2] Y. Ohno, D. K. Young, B. Beschoten, F. Matsukura, H. Ohno, and D. D. Awschalom, Nature (London) **402**, 790 (1999).
[3] T. Dietl, J. Appl. Phys. **89**, 7437 (2001).
[4] T. Dietl, H. Ohno, F. Matsukura, J. Cibert, and D. Ferrand, Science **287**, 1019 (2000).
[5] K. Ueda, H. Tabata, and T. Kawai, Appl. Phys. Lett. **79**, 988 (2001).
[6] H. Saeki, H. Tabata, and T. Kawai, Solid State Commun. **120**, 439 (2001).
[7] S. E. Park, H.-J. Lee, C. R. Cho, Y. C. Cho, S. Cho, and S.-Y. Jeong, Appl. Phys. Lett. **80**, 4187 (2002).
[8] Y. M. Cho, W. K. Choo, H. Kim, D. Kim, and Y. E. Ihm, Appl. Phys. Lett. **80**, 3358 (2002).
[9] Z. Jin, T. Fukumura, M. Kawasaki, K. Ando, H. Saito, T. Sekiguchi, Y. Z. Yoo, M. Murakami, Y. Matsumoto, T. Hasegawa, and H. Koinuma, Appl. Phys. Lett. **78**, 3824 (2001).
[10] K. Sato and H. Katayama-Yoshida, Jpn. J. Appl. Phys., Part 2 **40**, L334 (2001).
[11] C. D. Wagner, W. M. Riggs, L. E. Davis, and J. F. Moulder, in *Handbook of X-ray Photoelectron Spectroscopy*, edited by G. E. Mulenberg p. 78 (Perkin-Elmer Co., 1979), p. 78.
[12] S. A. Chambers, S. Thevuthasan, R. F. C. Farrow, R. F. Marks, J. U. Thiele, L. Folks, M. G. Samant, A. J. Kellock, N. Ruzycki, D. L. Ederer, and U. Diebold, Appl. Phys. Lett. **79**, 3467 (2001).
[13] J. H. Zhao, F. Matsukura, K. Takamura, E. Abe, D. Chiba, and H. Ohno, Appl. Phys. Lett. **79**, 2776 (2001).
[14] J. Ihm, A. Zunger, and M. L. Cohen, J. Phys. C **12**, 4409 (1979).
[15] N. Troullier and J. L. Martins, Phys. Rev. B **43**, 1993 (1991).
[16] S. B. Zhang, S.-H. Wei, and Alex Zunger, Phys. Rev. B **63**, 075205 (2001).
[17] H. Akai, Phys. Rev. Lett. **81**, 3002 (1998).